*Annals of Botany* **116**: 1023–1034, 2015
doi:10.1093/aob/mcv041, available online at www.aob.oxfordjournals.org

ANNALS OF BOTANY
Founded 1887

PART OF A SPECIAL ISSUE ON PLANTS AND CLIMATE CHANGE

# Modelling snow cover duration improves predictions of functional and taxonomic diversity for alpine plant communities

**Bradley Z. Carlson[1,2,*], Philippe Choler[1–5], Julien Renaud[1,2], Jean-Pierre Dedieu[6–8] and Wilfried Thuiller[1,2]**

*[1]Université Grenoble Alpes, LECA, F-38000 Grenoble, France, [2]CNRS, LECA, F-38000 Grenoble, France, [3]Université Grenoble Alpes, SAJF, F-38000 Grenoble, France, [4]CNRS, SAJF, F-38000 Grenoble, France, [5]LTER 'Zone Atelier Alpes', F-38000 Grenoble, France, [6]Université Grenoble Alpes, LTHE, F-38000 Grenoble, France, [7]CNRS, LTHE, F-38000 Grenoble, France and [8]IRD, LTHE, F-38000 Grenoble, France*
** For correspondence. E-mail brad.z.carlson@gmail.com*

Received: 7 December 2014 Returned for revision: 26 February 2015 Accepted: 3 March 2015 Published electronically: 7 April 2015

• **Background and Aims** Quantifying relationships between snow cover duration and plant community properties remains an important challenge in alpine ecology. This study develops a method to estimate spatial variation in energy availability in the context of a topographically complex, high-elevation watershed, which was used to test the explanatory power of environmental gradients both with and without snow cover in relation to taxonomic and functional plant diversity.
• **Methods** Snow cover in the French Alps was mapped at 15-m resolution using Landsat imagery for five recent years, and a generalized additive model (GAM) was fitted for each year linking snow to time and topography. Predicted snow cover maps were combined with air temperature and solar radiation data at daily resolution, summed for each year and averaged across years. Equivalent growing season energy gradients were also estimated without accounting for snow cover duration. Relationships were tested between environmental gradients and diversity metrics measured for 100 plots, including species richness, community-weighted mean traits, functional diversity and hyperspectral estimates of canopy chlorophyll content.
• **Key Results** Accounting for snow cover in environmental variables consistently led to improved predictive power as well as more ecologically meaningful characterizations of plant diversity. Model parameters differed significantly when fitted with and without snow cover. Filtering solar radiation with snow as compared without led to an average gain in $R^2$ of 0·26 and reversed slope direction to more intuitive relationships for several diversity metrics.
• **Conclusions** The results show that in alpine environments high-resolution data on snow cover duration are pivotal for capturing the spatial heterogeneity of both taxonomic and functional diversity. The use of climate variables without consideration of snow cover can lead to erroneous predictions of plant diversity. The results further indicate that studies seeking to predict the response of alpine plant communities to climate change need to consider shifts in both temperature and nival regimes.

**Key words:** Alpine grassland, climate change, French Alps, GAM, generalized additive model, growing season length, Landsat, mesotopography, plant community structure, remote sensing, snow cover.

## INTRODUCTION

In alpine landscapes, variation in snow cover duration along elevation and mesotopographic gradients has long been recognized as a key environmental filter structuring patterns of plant distribution and community composition (Billings, 1973; Evans *et al*., 1989). Snowpack affects the functioning of alpine ecosystems by exerting strong regulatory control on near-surface soil temperature (Edwards and Cresser, 1992), water and nutrient availability (Freppaz *et al*., 2007; Weingartner *et al*., 2007), plant growth and phenology (Kudo and Hirao, 2006; Wipf *et al*., 2009), growing season length and gross primary production (Baptist and Choler, 2008). Snowmelt timing has also been related to consistent shifts in alpine plant functional traits (Choler, 2005; Venn *et al*., 2011). Certain late-melting sites, for example, while limited by a short growing season, benefit from decreased exposure to frigid air temperatures in the winter and spring as well as increased water and nitrogen availability at the time of snow melt (Björk and Molau, 2007), and are identified as taxonomically distinct snowbed communities with particular functional traits, including low stature, high nitrogen leaf content per unit of mass and high specific leaf area (Choler, 2005). In the Alps, altered snow cover regimes in the form of earlier melt dates and rising snow lines have been observed during recent decades, and are anticipated to be an important ongoing consequence of climate change in alpine environments (Beniston, 2012). Collectively, this evidence highlights the importance of better understanding the linkages between snow cover regimes and plant diversity in order to improve models of alpine biodiversity in response to climate change.

Recognizing the importance of snow in alpine systems and building upon a naturalist tradition of field observations and

descriptive studies (e.g. Walker *et al*., 1993), several authors have incorporated snow as an explanatory variable with the goal of improving species distribution models (Heegaard, 2002; Odland and Munkejord, 2008; Randin *et al*., 2009; Schöb *et al*., 2009). Previous studies connecting plant occurrence or traits to snow-melt gradients have quantified snow cover duration by snowmelt rank (e.g. Heegaard, 2002), or by the first snow-free Julian day (e.g. Choler, 2005). Additionally, species distribution modelling studies focused on alpine plants have routinely estimated growing season length-related energy variables (e.g. solar radiation and growing degree days), without considering the mediating effect of snow cover duration on incoming solar radiation or near-surface air temperature (e.g. Zimmermann and Kienast, 1999; Randin *et al*., 2009; Carlson *et al*., 2014), which may lead to unrealistic estimates of energy availability for plants (Scherrer and Körner, 2011; Ford *et al*., 2013).

One consistent difficulty shared by plant ecologists seeking to take snow into account involves mapping and quantifying snow cover duration at sufficiently fine grain to represent meso-topographic heterogeneity (<50 m). Approaches used thus far have been based on manual field surveys (Heegaard, 2002; Choler, 2005; Odland and Munkejord, 2008; Schöb *et al*., 2009), *in situ* repeat photography (Scherrer and Körner, 2011) and at least one application of a mechanistic model of snow redistribution by wind (Randin *et al*., 2009). Process-based models accounting for meteorological forcing, topography and land cover have been developed and applied to forecast the effect of anticipated climate change on water budgets in mountainous environments (Liston and Elder, 2006; Viviroli *et al*., 2009; Vionnet *et al*., 2014). Validation of snow cover maps generated by two state-of-the-art hydrological models (Liston and Elder, 2006; Viviroli *et al*., 2009) relative to classified high-resolution imagery, however, showed fairly weak spatial agreement of snow-covered pixels during the snowmelt period (Randin *et al*., 2014; Table E.1), which is of critical interest to plant ecologists. Classification routines applied to Landsat imagery have long existed as tools for generating high-resolution snow cover maps at the regional scale (Dozier, 1989; Rosenthal and Dozier, 1996). Landsat images are freely available and have the added advantage of providing multiple scenes during the spring and summer months.

Here we implement a remote sensing-based framework for high-resolution mapping of snow cover duration that can be applied to larger extents than would be feasible with a field-mapping approach. While acknowledging the merits of a physical model of snow distribution (Randin *et al*., 2009), we present our approach as an empirical alternative for snow distribution modelling at the mesotopographic scale. In this study, our goal was to investigate the importance of snow cover duration for predicting multiple facets of plant community structure, including both trait-based and taxonomic diversity. At the scale of a 6·7-km$^2$ alpine basin, we mapped snow cover at 15-m resolution for five snowmelt cycles using Landsat imagery, modelled daily snow melt relative to time and mesotopography and combined snow cover maps with air temperature and solar radiation maps at a daily time step and for all five years. Assuming that the presence of snow cancelled incoming solar radiation and maintained near surface air temperature at 0 °C, we averaged the sum of snow-free growing season days, frost days and solar radiation across years. Comparable energy budgets were also estimated without taking snow cover into account. We then analysed the statistical and ecological implications of snow for predicting taxonomic and functional diversity metrics for 100 vegetation plots, including species richness, Simpson index, species composition as measured by non-metric multidimensional scaling (NMDS) dissimilarity (Faith *et al*., 1987), community-weighted mean plant height, specific leaf area (SLA), hyperspectral-derived estimates of leaf chlorophyll content and functional diversity. While we focus here on predicting current patterns of alpine plant community structure, a secondary aim is to elucidate which predictive variable(s) may be the most ecologically meaningful for forecasting the response of alpine plant communities to climate change.

## MATERIALS AND METHODS

### *Study area and floristic data*

The study area consists of a 6·7-km$^2$ watershed, spanning an elevation range from 1980 to 3114 m a.s.l., situated in the Grand Galibier Massif of the south-western French Alps (Fig. 1). This area, referred to as the Vallon de Roche Noire, is located in the commune of Le Monêtier-les-Bains within the Ecrins National Park. Vegetation consists of a mosaic of heath, sub-alpine and alpine forb and graminoid communities. Summer grazing is limited to sheep and cattle from late July to mid-September. Comprehensive botanical relevés, including visual estimates of species' relative abundance (Braun-Blanquet, 1957), were carried out for 90 plots of radius 2–5 m in July 2007. Ten additional relevés were completed in July 2011, making a total of 100 plots available for this analysis (Fig. 1).

### *Measuring alpine plant community diversity*

For each plot, species richness and Simpson diversity were quantified based on the community relevé. We used NMDS (Kruskal, 1964) to estimate turnover in species composition across plots. Bray–Curtis dissimilarity was calculated between plots and the resulting dissimilarity matrix was used as an input for NMDS ordination (stress = 0·2). Twenty-five per cent quantiles of scores from the first axis were used to class plots into four distinct groups, based on their taxonomic dissimilarity.

Morphological plant functional traits, including plant height, SLA, leaf dry matter content and leaf nitrogen content were collected from several field campaigns carried out in the study area (Choler, 2005; Chalmandrier *et al*., 2014). To reduce the pervasive effects of intraspecific trait variability on diversity estimates (Albert *et al*., 2012), we only used trait measurements sampled above 1800 m a.s.l. Community-weighted mean (CWM; Garnier *et al*., 2007) trait values for each plot were calculated for SLA and plant height by summing species-level trait values weighted by the abundance of species in the community. Plots for which we lacked trait data for ≥20 % of relative community composition were excluded from the analysis, as recommended by Pakeman and Quested (2007), resulting in the exclusion of 31 plots. For each of the 69 remaining plots, functional diversity was estimated by (1) calculating Gower's distance between all species relative to plant height, SLA, leaf dry matter content and leaf nitrogen content and (2) calculating

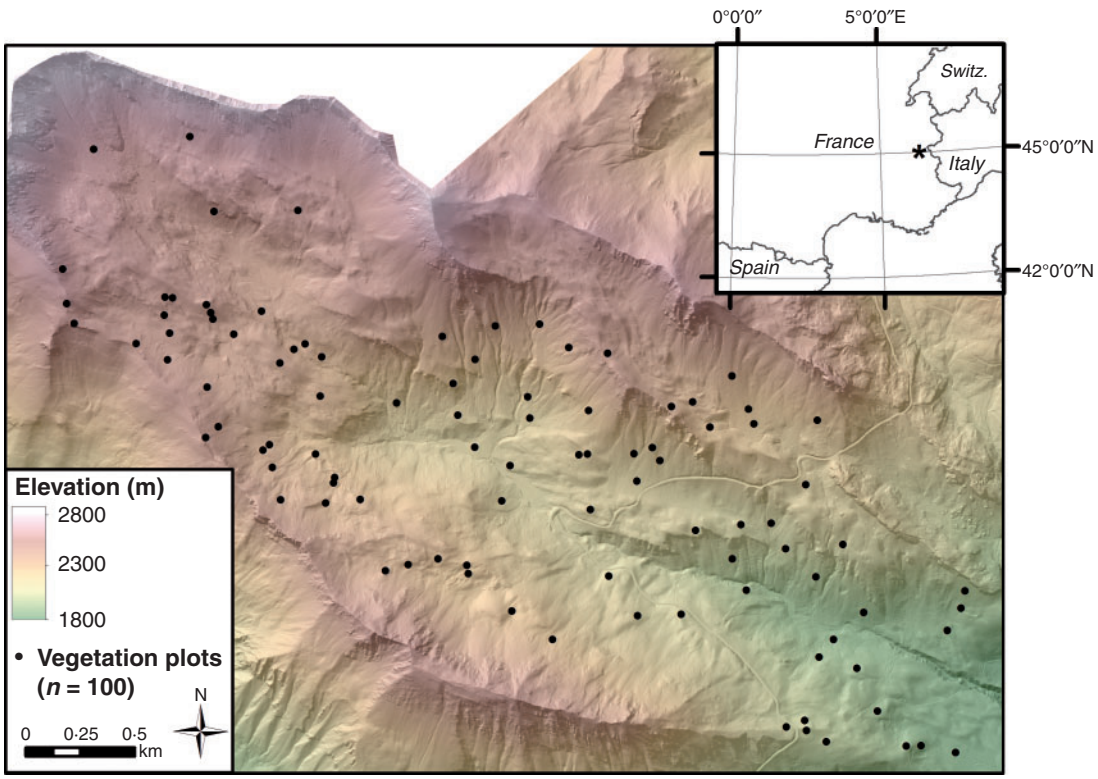


FIG. 1. Locator map for the study area displaying elevation and the location of vegetation plots. *Location of the study area in the inset map.

the abundance-weighted mean pairwise distance between all species in each plot using the mpd function in the picante R-package. Lastly, a community reshuffling routine that randomized species composition within plots while maintaining species richness was used to test whether convergence of functional diversity differed significantly from a null distribution following 1000 repetitions.

To complement field-based measures of plant diversity, leaf chlorophyll content ($a+b$; $\mu g\,cm^{-2}$) was extracted from a hyperspectral image (AISA; Specim Ltd., Finland) obtained for the study area in 2008. Leaf chlorophyll content estimated from reflectance values of hyperspectral imagery has been shown to be a reliable proxy for leaf nitrogen content (Haboudane *et al.*, 2002). Details concerning image acquisition and processing can be found in Pottier *et al.* (2014). The initial 0·8-m resolution image was resampled to 5 m using a mean function and values were extracted for each of the 100 vegetation plots.

### *Quantifying energy gradients*

Daily solar radiation values for 2013 were calculated with the area solar radiation tool in ArcGIS (version 10·2, 2013; Redlands, CA, USA) using a 2-m LiDAR digital elevation model and the clear sky model set to a sky size of 2800 pixels. Output solar radiation maps ($W\,m^{-2}$) for 2013 were used for corresponding calendar days in all other years, given that the underlying model did not account for inter-annual variation caused by nebulosity.

One-minute interval air temperature data for the Grand Galibier Massif was obtained by 300-m elevation class from the SAFRAN–Crocus–MEPRA model chain developed by Météo France. Details of data description, methodology and validation of this regional climate model for the French Alps are provided in Durand *et al.* (2009). Time series of air temperature for the years 2000–14 were aggregated to daily minimum ($T_{min}$) and mean ($T_{mean}$) values. Daily $T_{mean}$ values averaged across years were used to assess the potential length of the growing season, which was defined by the number of consecutive days with a mean temperature above 0 °C. The threshold of 0 °C was selected based on the minimum required temperature for alpine plant growth, as in Zimmermann and Kienast (1999). To add spatial grain, temperature values associated with a given elevation class (e.g. 2100–2400 m a.s.l.) were assigned to the median elevation (e.g. 2250 m a.s.l.) and elevation-dependent linear regression was used to downscale temperature values across the study area. Daily $T_{mean}$ and $T_{min}$ rasters were reclassified into binary maps, in which growing season days were defined as grid cells above 0 °C and frost days were defined as grid cells less than 0 °C. For each day falling within the potential estimated growing season and for five years (2000, 2001, 2002, 2013 and 2014), daily frost and growing season day maps were exported for the study area at 2-m resolution.

### *Snow cover mapping and modelling*

Landsat 7 (ETM+ sensor) imagery was obtained for five dates in 2000, five dates in 2001 and four dates in 2002. Landsat 8 (OLI sensor) was obtained for six dates in 2013 (Supplementary Data Fig. S1) and four dates in 2014.

All retained images had <30 % cloud cover and were acquired between late March and mid-August. Adequate imagery between 2003 and the commissioning of the Landsat 8 satellite in April 2013 was unavailable due to irreparable sensor damage to the Landsat 7 satellite occurring in the spring of 2003 (http://landsat.usgs.gov/). The panchromatic band 8 at 15-m resolution was selected for this analysis in order to maximize the resolution of snow cover maps. Scenes were re-projected to Lambert 93 and cropped to the study area prior to classification in eCognition Developer (version 8·0, 2012; Munich, Germany). Binary snow cover maps were generated first by segmenting the greyscale image according to the spectral values of the pixels and second by applying an object-based classification to the segmented image based on a nearest neighbour algorithm. Assignment of objects to snow or no snow classes took into account spectral signal values, as well as topographic context (slope and aspect). Given that available Landsat scenes did not always cover the end of the snow-melt cycle, a snow cover map derived from a 50-cm aerial photograph obtained on 6 August 2003 was aggregated to 15-m resolution using the majority parameter in ArcGIS and subsequently added to each annual Landsat time series. This additional step ensured that late summer snow patches, which occur in consistent locations in the study area from one year to the next (P. Choler, personal observation), were consistently documented.

Following data exploration, for each Landsat year a binomial generalized additive model (GAM; Wood, 2006) in the mgcv R package was used to relate the presence/absence of snow cover to temporal and topographic variables at 15-m resolution ($n = 654\,858$ grid cells). Restricted maximum likelihood was used to estimate penalized regression splines without a fixed number of degrees of freedom. Explanatory variables included: (1) calendar day; (2) solar radiation (estimated by calendar day); (3) normalized topographic position index (TPI; Wilson and Gallant, 2000) multiplied by slope for a 45-m moving window; (4) normalized TPI multiplied by slope for a 225-m moving window; and (5) mean annual temperature. Solar radiation was calculated using the same approach detailed above with a 15-m digital elevation model (DEM) as the input. We calculated TPI as a proxy for convexity and concavity relative to a neighbourhood of surrounding cells. Normalizing TPI values between 0 and 1 and multiplying this term by slope angle was intended to account for the expected increased likelihood of snow accumulation and persistence in low-angle, convex areas (Supplementary Data Fig. S2). The use of two different window sizes is supported by previous work (e.g. Revuelto *et al*., 2014) and was intended to quantify local topographic heterogeneity both in a local $3 \times 3$ ($45\,m^2$) grid cell neighbourhood and at the scale of a slope in a $15 \times 15$ ($225\,m^2$) neighbourhood. Mean annual temperature was estimated across the study area by (1) calculating mean annual temperature by elevation class from 2000 to 2013, (2) averaging mean annual temperature across years, and (3) applying elevation-dependent regression in order to provide continuous temperature predictions. In the GAM, mean annual temperature values were grouped by slope orientation category (N, NE, E, SE, S, SW, W and NW) and a response curve was fitted for each aspect class.

Fitted GAMs for each year were used to generate daily snow cover maps for five Landsat years (2000, 2001, 2002, 2013 and 2014). Although topographic variables remained constant, date and corresponding solar radiation varied by time step. Continuous probability of snow cover maps were converted to binary snow cover maps using the optimal threshold as determined by the true skill statistic (TSS) calculated between probability maps and observed snow cover maps (Allouche *et al*., 2006; Thuiller *et al*., 2009). Daily snow cover maps were exported for the five years at 15-m resolution.

### *Snow cover model validation*

SPOT 4 images were obtained for four additional dates in 2013 (www.cnes.fr). After correcting reflectance values for topography (Shepherd and Dymond, 2003), snow cover maps were generated at 20-m resolution by applying a threshold to the normalized difference snow index (NDSI; Dozier, 1989). SPOT 4 and Landsat-derived snow cover maps were resampled to a common 15-m resolution and compared with predicted GAM snow cover maps both (1) non-spatially, i.e. comparing estimates of percentage snow cover for the study area and (2) spatially, by applying the TSS (Allouche *et al*., 2006).

### *Combining snow cover with energy gradients*

For the length of the estimated growing season and for the five years considered, snow cover maps were combined with daily maps of air temperature and solar radiation. Snow cover maps were disaggregated to 2-m resolution to align with high-resolution maps and applied as a mask; e.g. if a grid cell contained snow, frost days, solar radiation and growing season days were set to zero. Temperature and solar radiation rasters were not upscaled to 15 m (the resolution of snow cover maps) in order to preserve variation in energy variables linked to finer topographic heterogeneity. Snow-free growing season days, frost days and solar radiation were summed for each grid cell and for each year, averaged across years and exported as 2-m raster layers. The sum of snow-free growing season days will be referred to from now on as growing season length (GSL). In addition to calculating average GSL across years, the variability in GSL was also estimated by extracting the range (maximum − minimum) of GSL from all five years and for each grid cell. This metric will be referred to as GSL variability. Solar radiation (for one year) and growing season length (for all five years, and then averaged) were also calculated by summing daily radiation and growing season day maps in the absence of snow cover.

### *Relating energy gradients to community properties*

Values for GSL and solar radiation with and without snow, GSL variability and snow-free frost days were extracted for each of the 100 vegetation plots and integrated into a common data table. Additionally, the percentage of bare ground at 5-m resolution was derived from a high-resolution aerial photograph using image segmentation and this information was extracted for each vegetation plot. We considered the percentage of bare ground to be a proxy for geomorphic disturbance related to slope and possible cryoturbation (Le Roux *et al*., 2013) and

also for biotic disturbance linked primarily to alpine marmot (*Marmota marmota*) activity (Choler, 2005).

To simplify parameter comparison across models, ordinary least squares linear regression was used to relate GSL and solar radiation with and without snow to taxonomic and functional diversity metrics. Model performance was measured by adjusted $R^2$ and mean absolute error (MAE). In the case of GSL and solar radiation filtered by snow cover, GSL variability, frost days and the percentage of bare ground were tested as explanatory variables against linear model residuals. Predictors explaining a significant portion of model residuals were retained and the best multivariate model (taking into account possible interaction effects) was fitted to each of the seven biodiversity metrics tested (species richness, Simpson index, NMDS dissimilarity, CWM plant height, CWM SLA, functional diversity and hyperspectral-based leaf chlorophyll content). Finally, to test for spatial patterns in diversity metrics not explained by selected input variables, Moran's $I$ was systematically used to test for spatial autocorrelation among residuals of the best-fitting model.

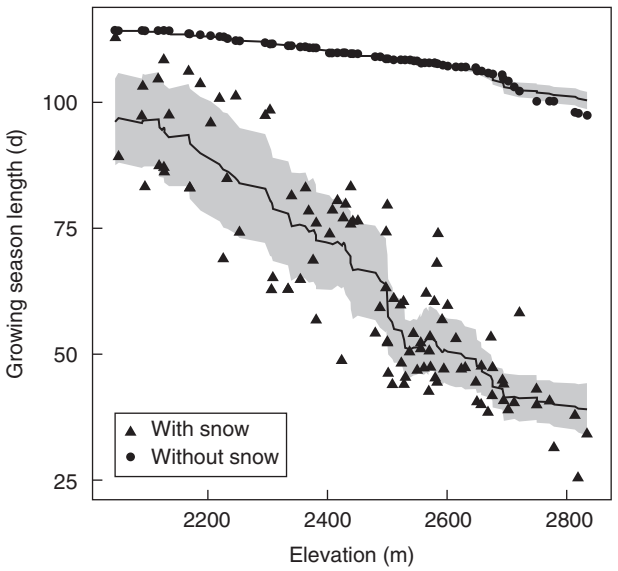


FIG. 2. Variation in growing season length relative to elevation estimated with and without snow cover (as indicated in key). Trend lines represent the running mean ($k = 20$), while the shaded ribbon represents the running mean ± the running mean absolute error ($k = 20$).

## RESULTS

### *Snow cover model validation*

Model performance for snow cover GAMs was consistent across years, with adjusted $R^2$ varying from 0·75 to 0·81 and explained deviance varying from 71 to 81 %. Comparison of estimates of relative snow cover area across the study site for seven dates in 2013 showed strong agreement between observed snow cover maps derived from Landsat 8 and SPOT imagery with GAM model outputs (MAE = 6·02 %, $R^2 = 0{\cdot}94$, $P < 0{\cdot}001$; Supplementary Data Fig. S3A, B). Agreement estimated by TSS between observed and predicted snow cover maps was especially elevated up to mid-July (>0·50), followed by a decline in agreement after this date (mean TSS = 0·54; Fig. S3C). Sensitivity exhibited a similar pattern, with close to 100 % of true positives detected up to July 15 followed by decreasing precision during the second half of the snowmelt period (mean sensitivity = 0·68).

### *Quantifying energy gradients*

The maximum length of the potential alpine growing season based on inter-annual daily mean air temperatures was found to occur from 22 April to 7 November (Supplementary Data Fig. S4). Here we summed growing degree days and solar radiation from 22 April to 15 August as the length of the initial period of growth has been shown to be a primary factor driving plant phenology and growth in alpine systems (Wipf *et al.*, 2009). Growing season length in this case is defined by relative differences in snowmelt timing prior to 15 August and therefore does not represent total energy received during the potential summer growing season.

Median differences in GSL and in the sum of solar radiation with and without snow cover duration were significant ($P < 0{\cdot}001$). When GSL was plotted against elevation, the standard error was substantially higher when snow cover was integrated (2·12 days compared with 0·38 days without snow), which was also the case for solar radiation (14 173 W m$^{-2}$ with snow compared with 6569 W m$^{-2}$ without). For a given elevation, the range of GSL with snow varied by up to 40 d, whereas without snow fluctuation in GSL relative to elevation was almost non-existent and could be attributed to inter-annual variability in daily air temperatures (Fig. 2). The Supplementary Data include a video file illustrating the combination of daily snow cover and solar radiation maps for 2013.

### *Relating energy gradients to community properties*

Due to strong co-linearity between solar radiation and GSL estimated with snow cover (Pearson's $r = 0{\cdot}96$), energy gradients were analysed separately in relation to plant community properties. Pearson's $r$ estimated between GSL and solar radiation without snow was substantially weaker ($r = -0{\cdot}32$). For GSL estimated with snow cover, adjusted $R^2$ increased and mean absolute error decreased for all taxonomic and functional diversity metrics, with the exception of leaf chlorophyll content (Table 1). While average gain in explanatory power when snow cover was taken into account was 3–4 %, increase in $R^2$ was particularly pronounced for community-weighted mean plant height (+0·20) and for functional diversity (+0·10; Table 1). Slope estimates were consistently lower and intercept values were consistently higher for GSL with snow cover compared with the absence of snow cover (Table 1; Fig. 3). For the seven diversity metrics considered, 95 % confidence intervals for parameter estimates (slope and intercept) did not overlap across models fitted to gradients with and without snow cover (Table 1).

For solar radiation, pronounced shifts in both explanatory power and the direction of relationships occurred. Whereas solar radiation exhibited no significant relationship with the

TABLE 1. *Linear model parameters, including 95 % confidence intervals and performance measures (adjusted* $R^2$ *and MAE) for gradients estimated with (S) and without (NS) snow*

| | | Taxonomic ($n = 100$) | | Functional | | | | |
|---|---|---|---|---|---|---|---|---|
| | | Richness | Simpson index | NMDS | Height ($n = 98$) | SLA ($n = 95$) | Functional diversity ($n = 67$) | Chlorophyll ($n = 74$) |
| GSL (S) | Intercept, estimated | 10·933 | 0·760 | 0·507 | –1·933 | 11·712 | 0·052 | 17·952 |
| | Intercept, lower | 5·529 | 0·730 | 0·429 | –4·373 | 10·169 | 0·040 | 4·562 |
| | Intercept, upper | 16·337 | 0·791 | 0·585 | 0·507 | 13·255 | 0·065 | 31·342 |
| | Slope, estimated | 0·288 | 0·001 | $-7{\cdot}78 \times 10^{-3}$ | 0·196 | 0·035 | $7{\cdot}56 \times 10^{-4}$ | 0·296 |
| | Slope, lower | 0·208 | 0·001 | $-8{\cdot}94 \times 10^{-3}$ | 0·160 | 0·012 | $5{\cdot}70 \times 10^{-4}$ | 0·113 |
| | Slope, upper | 0·368 | 0·002 | $-6{\cdot}62 \times 10^{-3}$ | 0·231 | 0·057 | $9{\cdot}43 \times 10^{-4}$ | 0·478 |
| | MAE | 6·673 | 0·035 | 0·096 | 2·804 | 1·784 | 0·012 | 11·008 |
| | $R^2$ (adjusted) | 0·334*** | 0·292*** | 0·641*** | 0·543*** | 0·080** | 0·495*** | 0·114** |
| GSL (NS) | Intercept, estimated | –128·947 | –0·056 | 4·523 | –84·062 | –4·082 | –0·335 | $^{-3}$36·700 |
| | Intercept, lower | –178·584 | –0·316 | 3·804 | –110·305 | –17·904 | –0·467 | –472·083 |
| | Intercept, upper | –79·311 | 0·205 | 5·243 | –57·820 | 9·741 | –0·202 | –201·309 |
| | Slope, estimated | 1·147 | $8{\cdot}37 \times 10^{-3}$ | –0·042 | 0·871 | 0·166 | $4{\cdot}0 \times 10^{-3}$ | 3·410 |
| | Slope, lower | 1·000 | $5{\cdot}97 \times 10^{-3}$ | –0·048 | 0·630 | 0·039 | $2{\cdot}79 \times 10^{-3}$ | 2·181 |
| | Slope, upper | 1·913 | $10{\cdot}8 \times 10^{-3}$ | –0·035 | 1·112 | 0·293 | $5{\cdot}22 \times 10^{-3}$ | 4·640 |
| | MAE | 7·787 | 0·035 | 0·096 | 3·530 | 1·801 | 0·013 | 9·914 |
| | $R^2$ (adjusted) | 0·283*** | 0·324*** | 0·609*** | 0·342*** | 0·057* | 0·390*** | 0·288*** |
| Solar (S) | Intercept, estimated | 13·549 | 0·771 | 0·438 | –0·763 | 11·137 | 0·056 | 25·270 |
| | Intercept lower | 8·174 | 0·741 | 0·353 | $^{-3}$·164 | 9·731 | 0·044 | 12·040 |
| | Intercept upper | 18·924 | 0·800 | 0·523 | 1·639 | 12·543 | 0·068 | 38·500 |
| | Slope, estimated | $3{\cdot}88 \times 10^{-5}$ | $2{\cdot}03 \times 10^{-7}$ | $-1{\cdot}05 \times 10^{-6}$ | $2{\cdot}79 \times 10^{-5}$ | $6{\cdot}817 \times 10^{-6}$ | $1{\cdot}073 \times 10^{-7}$ | $3{\cdot}00 \times 10^{-5}$ |
| | Slope lower | $2{\cdot}63 \times 10^{-5}$ | $1{\cdot}35 \times 10^{-7}$ | $-1{\cdot}25 \times 10^{-6}$ | $2{\cdot}23 \times 10^{-5}$ | $3{\cdot}596 \times 10^{-6}$ | $7{\cdot}96 \times 10^{-8}$ | $1{\cdot}848 \times 10^{-6}$ |
| | Slope upper | $5{\cdot}13 \times 10^{-5}$ | $2{\cdot}71 \times 10^{-7}$ | $-8{\cdot}57 \times 10^{-7}$ | $3{\cdot}41 \times 10^{-5}$ | $1{\cdot}004 \times 10^{-5}$ | $1{\cdot}35 \times 10^{-7}$ | $5{\cdot}810 \times 10^{-5}$ |
| | MAE | 6·953 | 0·036 | 0·107 | 2·941 | 1·705 | 0·012 | 10·894 |
| | $R^2$ (adjusted) | 0·273*** | 0·257*** | 0·531*** | 0·505*** | 0·151*** | 0·471*** | 0·046* |
| Solar (NS) | Intercept, estimated | 60·842 | 0·941 | –0·617 | 13·897 | 2·696 | 0·099 | 113·500 |
| | Intercept, lower | 38·285 | 0·816 | –1·059 | 1·357 | –2·328 | 0·025 | 69·508 |
| | Intercept, upper | 83·399 | 1·066 | –0·174 | 26·438 | 7·721 | 0·174 | 157·568 |
| | Slope, estimated | $-4{\cdot}28 \times 10^{-5}$ | $-1{\cdot}19 \times 10^{-7}$ | $8{\cdot}50 \times 10^{-7}$ | $-4{\cdot}37 \times 10^{-6}$ | $1{\cdot}531 \times 10^{-5}$ | 1·62 × 10–9 | –1·02 × 10–4 |
| | Slope, lower | $-7{\cdot}33 \times 10^{-5}$ | $-2{\cdot}88 \times 10^{-7}$ | $2{\cdot}51 \times 10^{-7}$ | $-4{\cdot}37 \times 10^{-6}$ | $8{\cdot}504 \times 10^{-6}$ | $-9{\cdot}80 \times 10^{-8}$ | –1·61 × 10–4 |
| | Slope, upper | $-1{\cdot}22 \times 10^{-5}$ | $5{\cdot}066 \times 10^{-8}$ | $1{\cdot}45 \times 10^{-7}$ | $-4{\cdot}37 \times 10^{-6}$ | $2{\cdot}211 \times 10^{-5}$ | $1{\cdot}01 \times 10^{-7}$ | $-4{\cdot}19 \times 10^{-6}$ |
| | MAE | 7·745 | 0·041 | 0·160 | 4·132 | 1·572 | 0·018 | 10·418 |
| | $R^2$ (adjusted) | 0·064** | 0·009 | 0·065** | –0·008 | 0·168*** | –0·015 | 0·126** |

*P* values: * $P < 0{\cdot}05$, ** $P < 0{\cdot}01$, *** $P < 0{\cdot}001$.
NMDS, scores from the first axis of NMDS ordination; SLA, community-weighted mean specific leaf area.

Simpson index, plant height or functional diversity, these relationships became highly significant when snow cover was added (Table 1; Fig. 4C, D). Although the direction of relationships remained positive both with and without snow, substantial gains in $R^2$ occurred when snow was included with respect to species richness (+0·21) and relative to first-axis NMDS scores (+0·51). Shifts in $R^2$ corresponded with changes of similar magnitude in mean absolute error (Table 1). Negative slope values estimated without snow for species richness, Simpson index, plant height and leaf chlorophyll content switched to being positive with snow, whereas the relationship between solar radiation and NMDS taxonomic dissimilarity changed from being positive to negative when snow was taken into account (Table 1; Fig. 4C, F). Explanatory power was slightly higher for SLA without snow (+0·02); however, mean absolute error was the same for both models. Within the 95 % quantile of SLA, snow bed plots expected to receive low solar radiation and exhibit high SLA were differentiated with snow (Fig. 4A), while these plots were scattered and poorly characterized when solar radiation was summed without snow cover (Fig. 4B). As was the case for GSL, 95 % confidence intervals for slope and intercept estimates for models with and without snow cover did not overlap (Table 1).

### *Analysis of residuals*

Overall, model residuals for solar and GSL responded in an equivalent manner with respect to other estimated environmental gradients (physical disturbance, frost stress and inter-annual variability in GSL), although $R^2$ was slightly higher for predictors applied to solar radiation residuals (Table 2). Accordingly, results for the two will be reported simultaneously. Physical disturbance explained a significant portion of residual variation for all taxonomic diversity metrics (Table 2). To a lesser degree, physical disturbance also captured variation in residuals for SLA and leaf chlorophyll content, but not for height or functional diversity. The estimated number of snow-free frost days was not a significant predictor of residual error for diversity metrics, with the exception of a weak relationship with plant height residuals in the case of solar radiation. Inter-annual variability in GSL was a significant predictor of model residuals in

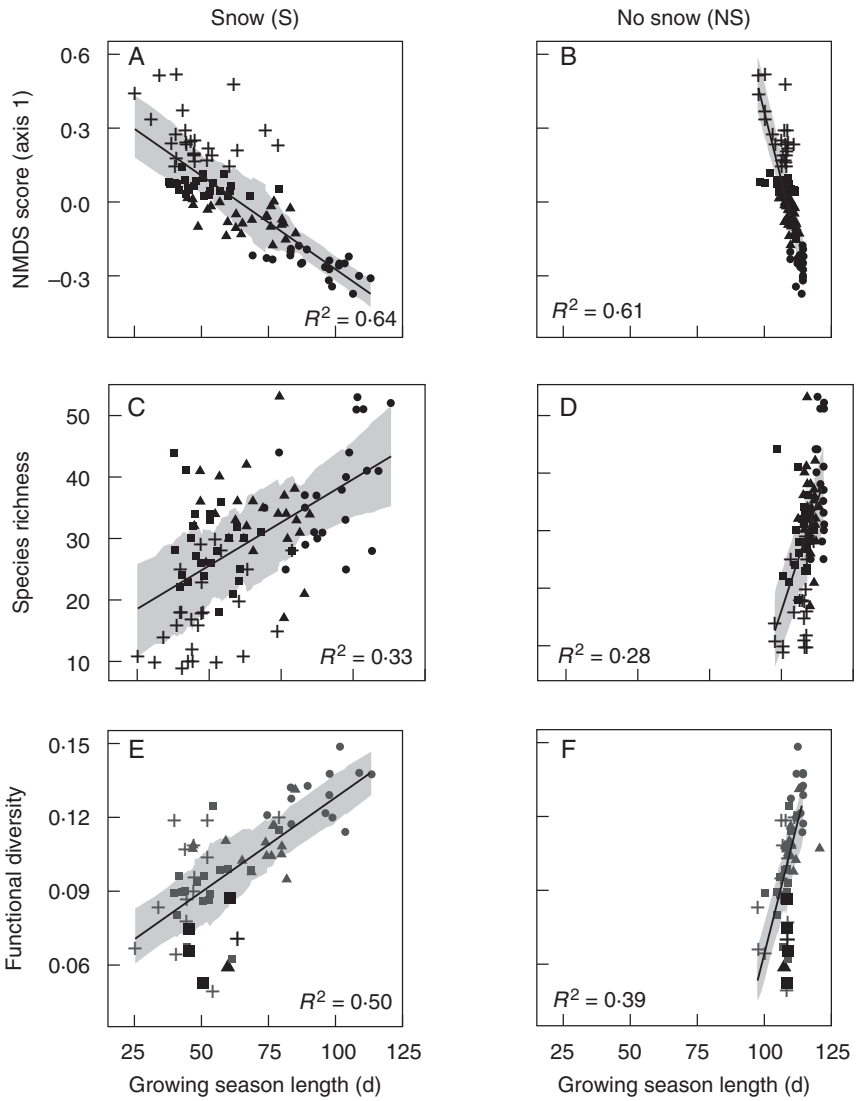


FIG. 3. First-axis NMDS score (A, B), species richness (C, D) and functional diversity (E, F) plotted relative to growing season length estimated with (left) and without (right) snow cover. Point symbols correspond to quartiles of the NMDS score. Black points in (E) and (F) represent significant functional convergence. Shaded ribbons correspond to the linear model ± the running mean absolute error ($k = 25$).

the case of species richness, NMDS dissimilarity, plant height, SLA and leaf chlorophyll content, but not for Simpson index or functional diversity (Table 2). GSL variability was greatest for high-elevation, south-facing scree communities, characterized by *Ranunculus glacialis* and *Oxyria digyna*.

Model residuals were not found to be spatially autocorrelated for gradients estimated with snow cover (Table 2). When snow cover was not taken into account, however, residuals were spatially autocorrelated for both GSL and solar radiation in the case of NMDS dissimilarity and plant height (results not shown), even when other predictors were incorporated in the model (bare ground and GSL variability). The lack of spatial autocorrelation when snow was included indicates that remaining unexplained variance in diversity metrics was due to local heterogeneity not accounted for in the model rather than systematic error in the estimation of energy availability. Finally, adjusted $R^2$ for the best-fitting multivariate model was equivalent or slightly higher in the case of GSL compared with solar radiation, with the exception of SLA, for which the solar radiation model captured 4 % more variation (Table 2). Averaging $R^2$ across diversity metrics, the multivariate GSL model was able to explain 56 % of variation in taxonomic diversity and 38 % of variation in functional diversity. In comparison, the solar radiation model captured slightly less (51 %) of the variation in taxonomic diversity and an equivalent amount (37 %) of the variation in functional diversity.

## DISCUSSION

Although previous studies have examined relationships between snow cover and alpine plant distribution patterns (Heegaard, 2002; Odland and Munkejord, 2008; Randin *et al.*, 2009; Schöb *et al.*, 2009) and functional traits (Choler, 2005;

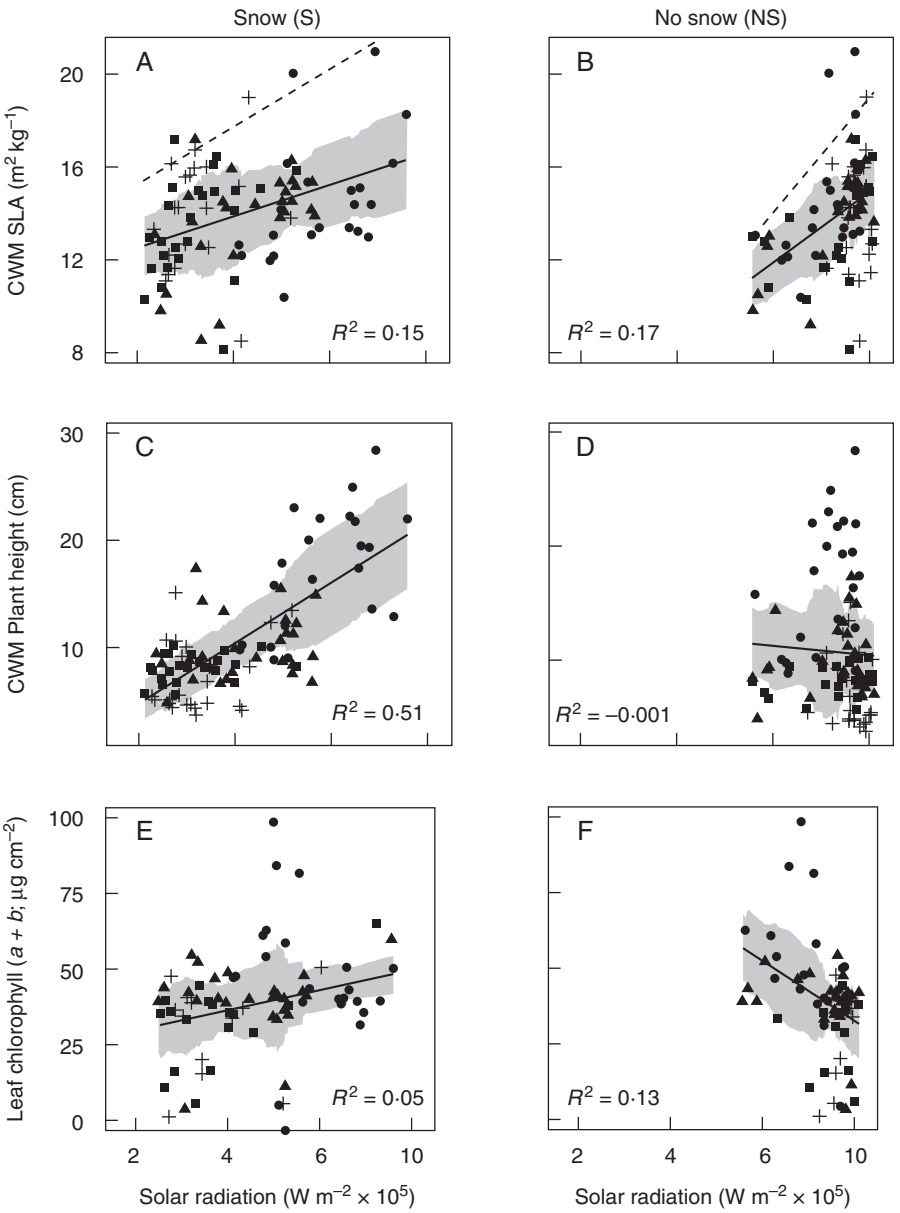


FIG. 4. CWM SLA ($m^2\,kg^{-1}$; A, B), CWM plant height (C, D) and percentage leaf chlorophyll content ($W\,m^{-2} \times 10^5$; E, F) plotted relative to the sum of solar radiation ($W\,m^{-2}$) estimated with (S) and without (NS) snow cover. Point symbols correspond to quartiles of the NMDS score. Shaded ribbons correspond to the linear model ± the running mean absolute error ($k = 25$). In (A) and (B), dashed lines represent the best fit regression applied to the 95 % quantile of CWM SLA values.

Venn *et al*., 2011), to the best of our knowledge this study is the first to quantitatively assess the importance of snow cover duration for predicting multiple facets of alpine plant diversity and structure along environmental gradients at the community level. Methodologically, we used a combination of high-resolution remote sensing products, a digital elevation model and coarse-resolution gridded climate data to implement an empirical snow distribution model (see Appendix for further discussion of our method relative to other approaches). Conceptually, we show the enhanced ecological relevance and statistical predictive power of bioclimatic variables that combine energy inputs (temperature and solar radiation) with snow cover duration. Our findings furthermore indicate that, in addition to energy gradients, inter-annual variability in growing season length, as well as physical disturbance, have strong effects on alpine plant community properties. Despite the small extent (~7 $km^2$) of our study area, given the ubiquitous nature of snow cover throughout high-elevation systems (Billings, 1973), we are confident that our findings are applicable to alpine areas in other geographic contexts.

### *Ecological and statistical contributions of integrating snow cover*

High variability in estimated growing season length for plots located at similar elevations but within contrasting

TABLE 2. *Residual variance explained (adjusted* $R^2$*) by disturbance (% bare ground), frost (number of snow-free frost days) and inter-annual growing season length (GSL) variation. Model performance (adjusted* $R^2$*) and results from Moran's* I *test are reported for the best model. Significant predictors of model residuals were included in the best model*

| | | Taxonomic | | Functional | | | | |
|---|---|---|---|---|---|---|---|---|
| | | Richness | Simpson | NMDS | Height | SLA | Functional diversity | Chlorophyll |
| GSL | Residual $R^2$ (disturbance) | 0·098*** | 0·211*** | 0·240*** | –0·002 | 0·055* | 0·005 | 0·054* |
| | Residual $R^2$ (frost) | –0·01 | 0·009 | –0·001 | 0·024 | –0·002 | –0·015 | 0·026 |
| | Residual $R^2$ (variation) | 0·079** | –0·009 | 0·069* | 0·079* | 0·060** | –0·013 | 0·041* |
| | Moran's *I* (*P* value) | 0·305 | 0·901 | 0·116 | 0·725 | 0·359 | 0·121 | 0·95 |
| | $R^2$ (best model) | 0·434*** | 0·467*** | 0·768*** | 0·534*** | 0·291*** (x) | 0·495*** | 0·213*** |
| Solar | Residual $R^2$ (disturbance) | 0·123*** | 0·236*** | 0·257*** | –0·008 | 0·047* | 0·009 | 0·065* |
| | Residual $R^2$ (frost) | –0·004 | 0·002 | –0·009 | 0·030* | –0·011 | –0·014 | –0·005 |
| | Residual $R^2$ (variation) | 0·158*** | 0·008 | 0·197*** | 0·037* | 0·053* | 0·012 | 0·086** |
| | Moran's *I* (*P* value) | 0·333 | 0·917 | 0·131 | 0·462 | 0·453 | 0·131 | 0·709 |
| | $R^2$ (best model) | 0·434*** | 0·456*** | 0·744*** | 0·525*** | 0·332*** (x) | 0·471*** | 0·195*** |

*P* values: * $P < 0·05$, ** $P < 0·01$, *** $P < 0·001$.
(x) denotes an interaction effect between solar/GSL and GSL variation (all other multivariate combinations are additive).
NMDS, scores from the first axis of NMDS ordination; SLA, community-weighted mean SLA.

mesotopographic contexts (Fig. 2) is in agreement with previous studies applying field-mapping techniques to differentiate environmental conditions for alpine plant communities (Walker *et al*., 1993; Choler, 2005). Our remote-sensing approach thus provides a spatially continuous method for estimating energy availability, which field measurements have shown is a strong driver of both community type and of aboveground phytomass production (Walker *et al*., 1994). Ideally, our estimate of growing season days would have been conducted using plot-level measures from *in situ* soil data loggers in order to better approximate thermal conditions found in microhabitats (Scherrer and Körner, 2011; Slavich *et al*., 2014). These data were not available for all Landsat years, however. Furthermore, and particularly given the remote-sensing approach used here, we argue that it is worthwhile to test the utility of variables that are widely available and that can be applied more readily at broader spatial scales, such as regional or, in this case, massif-scale air temperature. The local meteorological model we used (Durand *et al*., 2009) is based on continuous measurements from multiple local weather stations, and the outputs by 300-m elevation class that we downscaled are finer than standard macroclimatic variables, such as WorldClim (Hijmans *et al*., 2005). In the case of solar radiation, simulating daily clear sky gain in a GIS appears to be the best approach, given the difficulty and cost of instrumentation and the impracticality of interpolating point measurements. In summary, we consider that both GSL and solar radiation filtered by snow cover duration represent good proxies of energy availability, providing a more realistic estimate of conditions experienced by plant communities compared with thermal gradients estimated independently of snow cover duration. Furthermore, our selection of environmental variables based on ecological significance, e.g. plants only receiving radiation in the absence of snow, represents an important change in approach relative to modelling studies that frequently select predictors strictly on a statistical basis.

The comparatively strong statistical performance of GSL estimated without snow can be attributed to the underlying elevation gradient resulting from temperature downscaling. Despite the modest gain in explanatory power conferred by estimating GSL with snow cover (+3–4 %), the shift in model parameters (slope and intercept) emphasizes that snow cover had a strong effect on model fit. Furthermore, the more substantial 20 % gain in $R^2$ in the case of plant height suggests that energy availability estimated with snow better captures the environmental filter controlling variation in community-weighted mean plant height. By extension, the 10 % increase in $R^2$ relative to functional diversity is a strong indicator that functional convergence around an optimal trait in stressful conditions is better predicted when snow cover is taken into account (Table 1; Fig. 3E, F). As found in another study measuring leaf chlorophyll in the North American Rockies, we observed a decrease in leaf chlorophyll content with elevation (Spasojevic and Suding, 2012). However, high measured chlorophyll values for both *Vaccinium* sp.-dominated and *Festuca paniculata*-dominated communities, which are found at similar elevations but in opposite mesotopographic contexts, led to a decrease in $R^2$ for GSL with snow compared with the absence of snow (Table 1). This finding indicates that there may be a broad range of community-aggregated leaf trait values for a given level of snow cover duration.

Our findings strongly caution against the use of incident solar radiation summed without consideration of snow cover duration as a predictive variable for modelling studies in alpine environments. We found summer solar radiation estimated without snow to be a weak and at times misleading predictor of both functional and taxonomic diversity. The pronounced rise in $R^2$ for species richness, Simpson index, taxonomic dissimilarity (NMDS), plant height and functional diversity when snow was taken into account highlights the statistical gain afforded by summing snow-free incoming radiation during the growing season. Additionally, we found solar radiation summed without snow cover to be a significant *negative* predictor of species richness and leaf chlorophyll content. The switch to a more intuitive positive relationship between energy availability, photosynthetic activity and species richness points to the enhanced ecological significance gained by summing snow-free solar radiation.

While it has been demonstrated that community-weighted mean SLA declines with elevation (Bello *et al*., 2013) and that SLA increases in late-melting sites along a mesotopographic gradient (Choler, 2005), a third study shows that variation in community-weighted mean SLA measured in the context of a combined mesotopographic and elevation gradient exhibits no clear trend (Spasojevic and Suding, 2012). Although we found a significant relationship between SLA and solar radiation with and without snow (Table 1; Fig. 4A, B), consistently elevated mean absolute error points to the high range of SLA values for a given value of radiation throughout the gradient. We do not consider the $R^2$ value to be particularly meaningful in the case of SLA, given that previous studies have documented a wide range of community-weighted mean SLA values at high elevation in relation to snow cover duration (Choler, 2005). Diverging functional strategies, linked to fellfield and snowbed communities, are apparent at upper elevations when solar radiation is filtered by snow cover; however, this variation in the cold portion of the gradient is absent when received solar radiation is calculated in the absence of snow (Fig. 4A, B).

Despite the documented importance of frost events as a stress factor affecting the growth and survival of alpine plants (Körner, 2003; Wipf *et al*., 2006, 2009), our approach to summing snow-free frost days during the growing season did not constitute a significant predictor of model residuals (Table 2). We attribute this absence of explanatory power largely to a lack of measurement of sub-surface soil temperature not only during the winter months but also in spring, when plants are the most sensitive to snow-free frost damage (Bannister *et al*., 2005). Significant residual variance explained by physical disturbance, particularly in the case of taxonomic diversity (Table 1), however, confirms that the percentage of bare ground estimated from high-resolution imagery is a meaningful proxy for biotic and geomorphic disturbances affecting community composition.

Finally, while it is difficult to classify inter-annual variability in snow cover duration and air temperature as stress or disturbance (Grime, 1977), the amplitude of variation in GSL was a significant predictor of model residuals for the majority of diversity metrics considered (Table 2). A study conducted in Japan documents highly variable phenology of snowbed species relative to inter-annual variation in snow melt, whereas fellfield species initiated flowering and seed-set at consistent times regardless of melt date (Kudo *et al*., 2006). In addition to phenology, our findings support the conclusion that the taxonomic and functional characteristics of alpine grasslands are sensitive to the inter-annual consistency of snow cover duration, which has implications for ecosystem functioning (Baptist and Choler, 2008). Evidence from long-term monitoring of alpine plant communities' response to environmental change in the Colorado Rockies furthermore indicates that directional shifts in plant diversity are accompanied by fine-scale oscillations in community composition linked to inter-annual variability in environmental conditions, including snow cover duration (Spasojevic *et al*., 2013).

### *Implications for predicting community responses to climate change*

Our study, while focused on current patterns of alpine plant community properties, has strong implications for forecasting the response of alpine plants to global change. We view the shift in model parameters with and without snow as being of equivalent importance to the gain in explanatory power conferred by taking snow cover duration into account. More specifically, slope values were consistently higher when GSL was estimated without snow, which could lead to potentially extreme predictions of community responses to incremental climate change if snow cover is not taken into account.

As a next step emerging from this work, geared to linking energy availability to alpine plant diversity and functioning (phenology and productivity), we recommend summing received snow-free solar radiation when air temperature is above a physiologically meaningful threshold, such as 0 °C. Ecologically, this metric of energy availability would aim to quantify the amount of incoming solar radiation available for photosynthesis, as mediated by snow cover duration. Statistically, it would be possible to integrate available air temperature scenarios for the coming decades in order to define the potential growing season length (IPCC, 2007), even if clear-sky solar radiation remained constant for the prediction period. An ongoing challenge involves the procuring of future, climate-driven snow cover maps at appropriate spatial and temporal scales. Despite difficulties predicting persistent snow patches, recent studies demonstrate that forecasting the response of snow regimes to climate change is becoming increasingly feasible due to advances in hydrological modelling in mountainous study areas (Kobierska *et al*., 2013; Randin *et al*., 2014).

### *Conclusions*

While other studies have examined current patterns in order to infer the relevance of snow cover for predicting responses of alpine plants to global change (Bannister *et al*., 2005; Wipf *et al*., 2009; Venn *et al*., 2011), to the best of our knowledge ours is the first to demonstrate the utility of high-resolution imagery for mapping snow cover patterns in complex alpine terrain, and furthermore to provide a methodological framework for quantifying relationships between snow-mediated energy budgets and the multiple facets of taxonomic and functional diversity. The findings reported here underscore the importance of considering spatial heterogeneity in both thermal and nival regimes in order to link alpine plant community properties to environmental gradients, both for the present and in the context of global change.

## SUPPLEMENTARY DATA

Supplementary data are available online at www.aob.oxfordjournals.org and consist of the following. Figure S1: Landsat 8 scenes from 2013 cropped to the study area. Figure S2: combined slope and topographic position index maps derived for a 45-m moving window and for a 225-m moving window. Figure S3: observed and predicted snow cover area for 2013 Landsat and SPOT acquisition dates, and for the nine image acquisition dates. Agreement between observed and predicted snow cover area maps, and proportion of observed snow-covered pixels detected by the GAM model. Figure S4: daily mean air temperatures for the 2000–13 period. Video: animation of daily snow melt combined with daily maps of solar radiation (growing

season day 1 = 22 April 2013; growing season day 110 = 10 August 2013.

## ACKNOWLEDGEMENTS

We thank D. Georges, F. Mazel, L. Chalmandrier and C. Dentant for technical assistance and helpful discussions. Thanks are also due to T. Cavallo, who contributed results from the SPOT 4 – TAKE 5 Program. This research was conducted within the Long-Term Ecosystem Research (LTER) Zone Atelier Alpes, a member of the ILTER-Europe network. Data were provided in the context of the SPOT4-TAKE5 Program, initiated by the Centre d'Etudes Spatiales de la Biosphère (CESBIO) and which received additional funding from the Zone Atelier Alpes. The research leading to this paper received funding from the European Research Council under the European Community's Seven Framework Programme FP7/2007-2013 Grant Agreement no. 281422 (TEEMBIO).

## LITERATURE CITED

**Albert CH, de Bello F, Boulangeat I, Pellet G, Lavorel S, Thuiller W. 2012.** On the importance of intraspecific variability for the quantification of functional diversity. *Oikos* **121**: 116–126.

**Allouche O, Tsoar A, Kadmon R. 2006.** Assessing the accuracy of species distribution models: prevalence, kappa and the true skill statistic (TSS). *Journal of Applied Ecology* **43**: 1223–1232.

**Bannister P, Maegli T, Dickinson KJ, *et al.* 2005.** Will loss of snow cover during climatic warming expose New Zealand alpine plants to increased frost damage? *Oecologia* **144**: 245–256.

**Baptist F, Choler P. 2008.** A simulation of the importance of length of growing season and canopy functional properties on the seasonal gross primary production of temperate alpine meadows. *Annals of Botany* **101**: 549–559.

**Bello FD, Lavorel S, Lavergne S, *et al.* 2013.** Hierarchical effects of environmental filters on the functional structure of plant communities: a case study in the French Alps. *Ecography* **36**: 393–402.

**Beniston M. 2012.** Is snow in the Alps receding or disappearing? *Wiley Interdisciplinary Reviews: Climate Change* **3**: 349–358.

**Billings WD. 1973.** Arctic and Alpine vegetations: similarities, differences, and susceptibility to disturbance. *BioScience* **23**: 697–704.

**Björk RG, Molau U. 2007.** Ecology of alpine snowbeds and the impact of global change. *Arctic, Antarctic, and Alpine Research* **39**: 34–43.

**Braun-Blanquet J. 1957.** Ein Jahrhunder Florenwandel am Piz Linard (3414 m). *Bulletin du Jardin Botanique de l'Etat a Bruxelles*, Volume Jubilaire Walter Robyns: 221–232.

**Carlson BZ, Georges D, Rabatel A, *et al.* 2014.** Accounting for tree line shift, glacier retreat and primary succession in mountain plant distribution models. *Diversity and Distributions* **20**: 1379–1391.

**Chalmandrier L, Münkemüller T, Lavergne S, Thuiller W. 2014.** Effects of species' similarity and dominance on the functional and phylogenetic structure of a plant meta-community. *Ecology* **96**: 143–153.

**Choler P. 2005.** Consistent shifts in alpine plant traits along a mesotopographical gradient. *Arctic, Antarctic, and Alpine Research* **37**: 444–453.

**Dozier J. 1989.** Spectral signature of alpine snow cover from the Landsat Thematic Mapper. *Remote Sensing of Environment* **28**: 9–22.

**Durand Y, Laternser M, Giraud G, Etchevers P, Lesaffre B, Merindol L. 2009.** Reanalysis of 44 yr of climate in the French Alps (1958-2002): methodology, model validation, climatology, and trends for air temperature and precipitation. *Journal of Applied Meteorology and Climatology* **48**: 429–449.

**Edwards AC, Cresser MS. 1992.** Freezing and its effect on chemical and biological properties of soil. *Advances in Soil Science* **18**: 59–79.

**Evans BM, Walker DA, Benson CS, Nordstrand EA, Petersen GW. 1989.** Spatial interrelationships between terrain, snow distribution and vegetation patterns at an arctic foothills site in Alaska. *Ecography* **12**: 270–278.

**Faith DP, Minchin PR, Belbin L. 1987.** Compositional dissimilarity as a robust measure of ecological distance. *Vegetatio* **69**: 57–68.

**Ford KR, Ettinger AK, Lundquist JD, Raleigh MS, Lambers JHR. 2013.** Spatial heterogeneity in ecologically important climate variables at coarse and fine scales in a high-snow mountain landscape. *PLoS One* **8**: e65008.

**Freppaz M, Williams BL, Edwards AC, Scalenghe R, Zanini E. 2007.** Simulating soil freeze/thaw cycles typical of winter alpine conditions: implications for N and P availability. *Applied Soil Ecology* **35**: 247–255.

**Garnier E, Lavorel S, Ansquer P, *et al.* 2007.** Assessing the effects of land-use change on plant traits, communities and ecosystem functioning in grasslands: a standardized methodology and lessons from an application to 11 European sites. *Annals of Botany* **99**: 967–985.

**Grime JP. 1977.** Evidence for the existence of three primary strategies in plants and its relevance to ecological and evolutionary theory. *American Naturalist* **111**: 1169–1194.

**Haboudane D, Miller JR, Tremblay N, Zarco-Tejada PJ, Dextraze L. 2002.** Integrated narrow-band vegetation indices for prediction of crop chlorophyll content for application to precision agriculture. *Remote Sensing of Environment* **81**: 416–426.

**Heegaard E. 2002.** A model of alpine species distribution in relation to snowmelt time and altitude. *Journal of Vegetation Science* **13**: 493–504.

**Hijmans RJ, Cameron SE, Parra JL, Jones PG, Jarvis A. 2005.** Very high resolution interpolated climate surfaces for global land areas. *International Journal of Climatology* **25**: 1965–1978.

**IPCC. 2007.** *Climate change (2007): The physical science basis. Contribution of Working Group I to the Fourth Assessment Report of the Intergovernmental Panel on Climate Change*. Cambridge: Cambridge University Press.

**Kobierska F, Jonas T, Zappa M, Bavay M, Magnusson J, Bernasconi SM. 2013.** Future runoff from a partly glacierized watershed in central Switzerland: a 2 model approach. *Advances in Water Resources* **55**: 204–214.

**Körner C. (2003.** *Alpine plant life: functional plant ecology of high mountain ecosystems*. Heidelberg: Springer.

**Kruskal JB. 1964.** Nonmetric multidimensional scaling: a numerical method. *Psychometrika* **29**: 115–129.

**Kudo G, Hirao AS. 2006.** Habitat-specific responses in the flowering phenology and seed set of alpine plants to climate variation: implications for global-change impacts. *Population Ecology* **48**: 49–58.

**Liston GE, Elder K. 2006.** A distributed snow-evolution modeling system (SnowModel). *Journal of Hydrometeorology* **7**: 1259–1276.

**Odland, A, Munkejord HK. 2008.** Plants as indicators of snow layer duration in southern Norwegian mountains. *Ecological Indicators* **8**: 57–68.

**Pakeman RJ, Quested HM. 2007.** Sampling plant functional traits: what proportion of the species need to be measured? *Applied Vegetation Science* **10**: 91–96.

**Pottier J, Malenovský Z, Psomas A, *et al.* 2014.** Modelling plant species distribution in alpine grasslands using airborne imaging spectroscopy. *Biology Letters* **10**: 20140347.

**Randin CF, Vuissoz G, Liston GE, Vittoz P, Guisan A. 2009.** Introduction of snow and geomorphic disturbance variables into predictive models of alpine plant distribution in the Western Swiss Alps. *Arctic, Antarctic, and Alpine Research* **41**: 347–361.

**Randin CF, Dedieu JP, Zappa M, Long L, and Dullinger S. 2014.** Validation of and comparison between a semidistributed rainfall–runoff hydrological model (PREVAH) and a spatially distributed snow-evolution model (SnowModel) for snow cover prediction in mountain ecosystems, *Ecohydrology* in press. doi:10.1002/eco.1570.

**Revuelto J, López-Moreno JI, Azorín-Molina C, Vicente Serrano SM. 2014.** Topographic control of snowpack distribution in a small catchment in the central Spanish Pyrenees: intra-and inter-annual persistence. *Cryosphere* **8**: 1989–2006.

**Rosenthal W, Dozier J. 1996.** Automated mapping of montane snow cover at subpixel resolution from the Landsat Thematic Mapper. *Water Resources Research* **32**: 115–130.

**Le Roux PC, Virtanen R, Luoto M. 2013.** Geomorphological disturbance is necessary for predicting fine scale species distributions. *Ecography* **36**: 800–808.

**Scherrer D, Körner C. 2011.** Topographically controlled thermal-habitat differentiation buffers alpine plant diversity against climate warming. *Journal of Biogeography* **38**: 406–416.

**Schöb C, Kammer PM, Choler P, Veit H. 2009.** Small-scale plant species distribution in snowbeds and its sensitivity to climate change. *Plant Ecology* **200**: 91–104.

**Shepherd JD, Dymond JR. 2003.** Correcting satellite imagery for the variance of reflectance and illumination with topography. *International Journal of Remote Sensing* **24**: 3503–3514.

**Slavich E, Warton DI, Ashcroft MB, Gollan JR, Ramp D. 2014.** Topoclimate versus macroclimate: how does climate mapping methodology affect species distribution models and climate change projections? *Diversity and Distributions* **20**: 952–963.

**Spasojevic MJ, Suding KN. 2012.** Inferring community assembly mechanisms from functional diversity patterns: the importance of multiple assembly processes. *Journal of Ecology* **100**: 652–661.

**Spasojevic MJ, Bowman WD, Humphries HC, Seastedt TR, Suding KN. 2013.** Changes in alpine vegetation over 21 years: are patterns across a heterogeneous landscape consistent with predictions? *Ecosphere* **4**: art117. doi.org/10.1890/ES13-00133.1.

**Thuiller W, Lafourcade B, Engler R, Araujo MB. 2009.** BIOMOD – a platform for ensemble forecasting of species distributions. *Ecography* **32**: 369–373.

**Venn SE, Green K, Pickering CM, Morgan JW. 2011.** Using plant functional traits to explain community composition across a strong environmental filter in Australian alpine snowpatches. *Plant Ecology* **212**: 1491–1499.

**Vionnet, V, Martin E, Masson V, *et al.* 2014.** Simulation of wind-induced snow transport and sublimation in alpine terrain using a fully coupled snowpack/atmosphere model. *Cryosphere* **8**: 395–415.

**Viviroli D, Zappa M, Gurtz J, Weingartner R. 2009.** An introduction to the hydrological modelling system PREVAH and its pre-and post-processing-tools. *Environmental Modelling & Software* **24**: 1209–1222.

**Walker DA, Halfpenny JC, Walker MD, Wessman CA. 1993.** Long-term studies of snow-vegetation interactions. *BioScience* **43**: 287–301.

**Walker MD, Webber PJ, Arnold EH, Ebert-May D. 1994.** Effects of interannual climate variation on aboveground phytomass in alpine vegetation. *Ecology* **75**: 393–408.

**Weingartner R, Viviroli D, Schaedler B. 2007.** Water resources in mountain regions: a methodological approach to assess the water balance in a highland–lowland system. *Hydrological Processes* **21**: 578–585.

**Wilson JP, Gallant JC. 2000.** *Terrain analysis: principles and applications*. New York: John Wiley & Sons.

**Wipf S, Rixen C, Mulder CP. 2006.** Advanced snowmelt causes shift towards positive neighbour interactions in a subarctic tundra community. *Global Change Biology* **12**: 1496–1506.

**Wipf S, Stoeckli V, Bebi P. 2009.** Winter climate change in alpine tundra: plant responses to changes in snow depth and snowmelt timing. *Climatic Change* **94**: 105–121.

**Wood S. 2006.** *Generalized additive models: an introduction with R*. Boca Raton, FL: CRC Press.

**Zimmermann NE, Kienast F. 1999.** Predictive mapping of alpine grasslands in Switzerland: species versus community approach. *Journal of Vegetation Science* **10**: 469–482.

## APPENDIX. STRENGTHS AND LIMITATIONS OF THE SNOW DISTRIBUTION MODEL

Predicting snow height, snow water equivalent and snow distribution at spatial resolutions pertinent to mesotopographic variation in an alpine context (<50 m) constitutes an ongoing challenge in the realm of process-based climate and hydrological modelling (Vionnet *et al*., 2014). Mechanistic models have been developed for this purpose, taking into account meteorological forcing, land cover and topography [PREVAH (Viviroli *et al*., 2009)] and also snow redistribution by wind [SnowModel (Liston and Elder, 2006); Crocus (Vionnet *et al*. 2014)]. Such models are well suited to forecasting the effect of climate change on snow cover regimes (Kobierska *et al*., 2013), and have already been applied successfully to improve predictive variables in a species distribution modelling context (Randin *et al*., 2009). For the time being and from the standpoint of plant ecologists, however, we are not convinced that existing process-based models are superior to a remote sensing-based approach at <20-m resolution, particularly when the critical period of interest is the snow-melt cycle. A recent study comparing snow cover maps at 20-m resolution generated by SnowModel and PREVAH in the Austrian Alps to observed snow cover maps classified from SPOT imagery found low agreement during the melting period [5·4 % of true positives were detected in the case of PREVAH, and 10.1 % for SnowModel (Randin *et al*., 2014)]. Comparison of predicted snow cover maps with 2013 Landsat and SPOT imagery in this study, in contrast, yielded an average detection of 68 % of true positives during the melting period, although this rate did fall below 50 % after 15 July (Supplementary Data Fig. S3D). In short, while a process-based approach to snow modelling is ultimately the most desirable, we argue that the approach used here is viable for two principal reasons: (1) the spatial patchwork generated by snowmelt patterns is well captured by high-resolution imagery (Supplementary Data Fig. S1), allowing for simple modelling of a complex phenomenon; and (2) our approach is applicable by ecologists with access to high-resolution digital elevation data and Landsat imagery.

Despite a number of advantages, we are aware that our empirical approach to snow modelling is inadequate for precisely predicting end-of-season snow patches persisting until early August. Late-melting sites largely independent of elevation caused by snow accumulation due to avalanches, for example, were not captured by our model. While model performance remained high for the majority of the melt period from the end of April to mid-July (Supplementary Data Fig. S3A, B), the decline in spatial agreement at the end of summer compared with observed snow cover maps can be attributed to increasing relative importance of mesotopographic context and decreasing relative importance of date and elevation over the course of the melt cycle. Failure to account for this tendency in the model explains, at least in part, why the predicted ranking of snow melt by site differed for certain high-elevation plots from field observations. Although late July snow patches can affect the growing season length for certain nival species, such as *Doronicum grandiflorum* and *Geum reptans*, the first snow-free day for snow bed communities dominated by *Salix herbacea*, *Alchemilla pentaphyllea* and *Carex foetida* typically occurs before the beginning of July within the study area (Choler, 2005). The strong spatial agreement between observed and predicted snow cover maps up to 15 July therefore justifies the approach adopted here for modelling snowmelt patterns (Supplementary Data Fig. S3), and suggests that our method can be expected to perform well in the context of other alpine environments.